Jet-engine vibration model for the estimation of pylon-wing interface loads

Sebastian F. Zettel[1], Marc Böswald[1], René Winter[1]

[1] *Deutsches Zentrum für Luft- und Raumfahrt, Institut für Aeroelastik, Göttingen. Email: sebastian.zettel@dlr.de*

Introduction

Passengers in aircraft cabins experience noise impact from different sources. First, the turbulent boundary layer excites the cabin-structure due to air flow. Second, engines and sub-systems installed on and in the aircraft-structure transmit airborne noise into the cabin. Additionally, they induce vibrations which excite the cabin structure and result in noise. The main focus of this paper is the quantification of vibrations induced by jet-engines during cruising flight operation.

Currently, the German Aerospace Center (DLR) is actively working on two projects which introduce the requirement for a model that approximates the vibration loads applied to the interface between pylon (structure that connects jet-engine with airframe) and wing. In the DLR project "Intonate - Interior Noise and Vibration Validation" a digital analysis process is developed to allow to assess new aircraft concepts regarding their cabin acoustics based on numerical models during the design process. In order to simulate the most realistic cabin acoustics, all above mentioned sources of noise need to be considered. In the project *Large Passenger Aircraft IADP* within Clean Sky 2, the energy transfer of the wing caused by vibrations is investigated. The idea is to excite a real wing structure in a laboratory-like setup. The goals are to update a Finite Element Method (FEM) model but also to quantify the vibrational power flow which enters the cabin, based on wing vibrations excited at the engine attachment points on the wing.

The vibration characteristic of a jet-engine is a prerequisite for such a vibration. However, there is no jet-engine and no measurement data of its vibrations available. As a consequence, an attempt is made to develop an engine vibration model from minimal input data that allows the estimation of the interface loads at the engine attachment points. Bearing forces during regular (stationary) operation, engine layout data, in-flight data from measurements and a simple substitute model of an engine are combined for this. The basic idea for the engine model is to calculate the permissible unbalance forces of the engine and to apply these to a FEM model which geometrically represents the bearing locations in the jet-engine and the pylon. These unbalance forces induce vibrations into the engine structure which will be propagated through it, into the pylon and finally into the wing. Currently, only the unbalance forces acting perpendicular to the engine rotation axis are accounted for. Forces acting in the direction of the engine rotation axis are not incorporated.

In the following chapter *Estimation of Engine Vibrations* the estimation of engine vibrations and the considered frequencies for a realistic excitation are described. In the chapter *FEM Model & Results* the created substitute model and the considerations taken into account will be described as well as the resulting loads in the interface presented.

Estimation of Engine Vibrations

In order to estimate missing vibration data it is necessary to acquire data regarding unbalance forces in the engine as well as exact rotation speeds of low- and high-pressure shaft during operation. Additionally, it should be considered that during vibration measurements of actual mechanical systems there are usually sub- and higher harmonics present. If possible these harmonics should be considered in a model in order to represent the vibrations as realistic as possible.

Unbalance Forces in stationary operation

Rotors which operate at high rotation speeds need to be balanced in order to provide a reliable operation of the bearings and support structure in the envisaged fatigue life. The process to calculate necessary values for the balancing of rotors is described in the DIN Norm 1940 and its subsequent ISO standards [1]. After the balancing of rotors they have remaining unbalances which result in vibration during operation. However, these vibrations, as mentioned above, are on a level which do not negatively affect the operation of the system but can be tolerated.

Based on the system which needs to be balanced the mentioned DIN Norm 1940 gives guiding values for the unbalance quality, here stated as G $[mm \cdot s]$. For example the stated unbalance quality for jet-engines is $G = 6.3$ $mm \cdot s$. Based on this value and using the rotor mass m_{Rotor} [kg] and the maximum rotation speed of the rotor Ω $[\frac{1}{s}]$ the permitted remaining unbalance for one of the rotor bearings U_i can be calculated by (2)

$$U_\mathrm{i} = 1000 \cdot \frac{G \cdot m_\mathrm{Rotor}}{\Omega} \cdot k_\mathrm{i} \qquad [\mathrm{g \cdot mm}]. \quad (1)$$

The variable k_i stands for the load fraction of the current bearing. As rotors have at least two bearing the respective load fractions need to be calculated depending on the mass distribution of the rotor. Accordingly, the bearing distances and the position of the rotors center of gravity need to be known.

The resulting permitted unbalance forces can be calculated by (2)

$$F_\mathrm{i} = 10^{-6} \cdot U_\mathrm{i} \cdot \Omega^2 \qquad [\mathrm{N}]. \quad (2)$$

While this is the process to calculate the permitted unbalance forces of the rotor at the highest rotation speeds it is simply possible to use the rotations speeds of certain flight conditions to get the unbalance forces

which will act in the engine and induce vibrations throughout its structure as it is a linear scaling.

Within the project *Intonate* the respective values for masses, the bearing locations and maximum shaft rotation speeds were given in form of a engine layout data sheet for a V2500 jet-engine manufactured by *International Aero Engines AG*. This engine is used for the project due to the research aircraft *DLR ATRA* (Advanced Technology Research Aircraft) which is a research platform based on a Airbus A320. The installed engines are V2500s and accordingly relevant data is available.

Shaft speeds at common flight conditions
The rotation speeds of low- (N1) and high-pressure (N2) shafts of jet-engines are independent. The resulting rotation speeds are based on flight conditions and surrounding atmospheric parameters. This is the reason why it is not as easy to get the rotations speed of the two shafts of an engine for example at cruising flight. Most of the time in documents there are only maximum rotations speeds for both shafts stated.

In 2012 the DLR conducted a measurement campaign within the project *Simkab* using the research aircraft *DLR ATRA*. During this measurement an enormous amount of data regarding aircraft sensor data and vibroacoustics was acquired during in-flight conditions. Part of this data are the engine shaft rotation speeds as well as altitude and wind speed for full flights. Based on this data it was possible to identify the shaft rotation speeds for different flight conditions. As an example, during cruising flight (stationary flight speed at cruising altitude) the N1 shaft rotates at 76% and the N2 shaft at 83% of the respective maximum shaft rotation speeds. For safety related reasons the exact rotation speeds will not be stated.

Sub- and higher harmonics of jet engines
During the before mentioned measurement campaign on the DLR ATRA, accelerometers were installed on the fuselage near the wings. These captured the vibrations of the structure induced by a combination of sources like the turbulent boundary layer as well as the engines and subsystems. In the subsequent evaluation of the acquired data it was found that in a frequency range up to 300 Hz the accelerometers on the fuselage showed response peaks at the rotation speeds of the low- and high-pressure shafts [2]. Additionally, the data showed response peaks at one sub harmonic and one higher harmonic of the low pressure shaft, more precisely at 0.5 x f_{N1} and 2 x f_{N1}. Considering these harmonics of the low-pressure shaft in the jet-engine vibration model is thus important as these frequencies show impact on the cabin structure by propagating through the transfer path wing.

FEM Model & Results

This chapter covers the built-up FEM model to which the unbalance forces are applied (see chapter *Estimation of engine vibrations*). Additionally, illustrations of the engine-pylon-wing system and the resulting output of the model will be shown.

FEM Model
To give an overview, a basic setup of an engine attached to a wing utilizing a pylon is shown in Figure 1. There

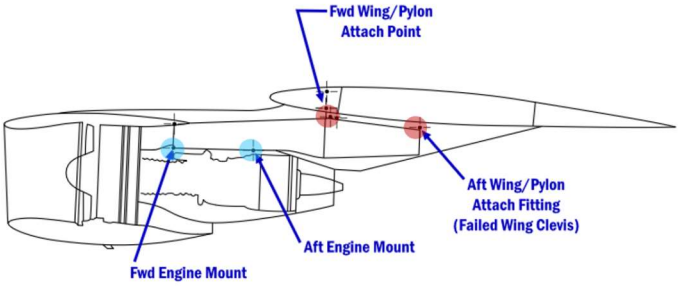

Figure 1: Engine-Pylon-Wing system overview with attachment point indicators, blue: engine to pylon attachment points, red: pylon to wing attachment points [3]

are two attachment points per interface with one interface between engine and pylon (EP-interface), and one interface between pylon and wing (PW-interface).

The attachment points in the above mentioned interfaces are not fully fixed points which transmit loads in all six degrees-of-freedom (DOF). The points in the front and back respectively transmit loads only in certain directions which are shown in Figure 2. In case of the attachment

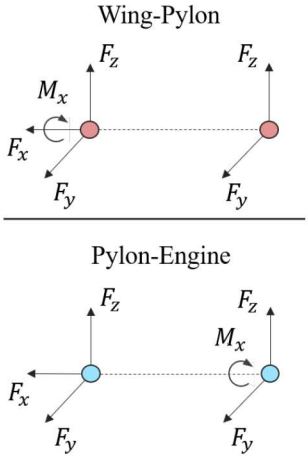

Figure 2: Transmitted loads in the engine-pylon and pylon-wing interfaces for the respective attachment points in the front and back for a Airbus A320 (Attachment points position in reference to Figure 1)

points in the PW-interface, the fixed DOF for the constraints are set accordingly. The attachment points in the EP-interface are modelled using rigid body elements (RBEs). These RBEs allow to specify the DOF for which loads are transmitted.

A cut through the engine core with indicators for bearing locations and the attachment locations in the EP-interface are shown in Figure 3. The V2500 jet-engine contains five bearing locations, three for the low-pressure shaft and two for the high-pressure shaft.

The FEM model used here includes a representation of the pylon based on a reference model from Airbus, see Figure 4a) and b). There was no model updating performed for the pylon model as no measurement data of a

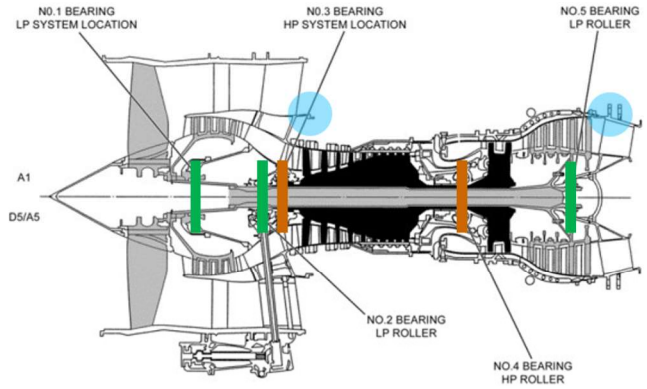

Figure 3: Jet-engine core cut with indicators for attachment points to pylon (blue) and bearing locations, green: low-pressure shaft, orange: high-pressure shaft [4]

respective pylon is available yet. However, it is assumed that the reference model, on which the here seen model is based on, provides a realistic representation. The main part of the pylon is a box structure modelled with shell elements. Additionally, in the front of the pylon there is a small frame structure to which creates the forward attachment point in the EP-interface. The engine itself is represented by a simple frame structure in the form of stiff bars connecting the individual bearing locations with the two attachment points in the EP-interface, see Figure 4 c) in comparison to a) and b). As there is no in-

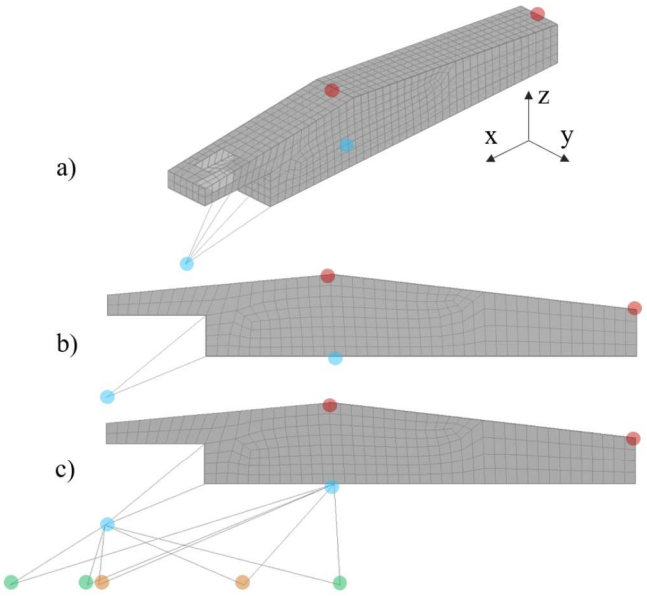

Figure 4: Substitute engine-pylon model, a) isometric view without engine, b) side view without engine, c) side view with substitute engine

formation regarding the structural characteristics of the core engine, the bars were assigned an artificially high stiffness. The eigenfrequencies of the engine part of the model lay outside the considered frequency range of 500 Hz. The cut-off frequency is chosen at 500 Hz as previous studies showed that cabin acoustics in terms of vibroacoustics show the biggest impact up to 300 - 500 Hz [5]. Above this range the turbulent boundary layer starts to have more impact on cabin acoustics.

The calculated unbalance forces (calculated for every individual bearing) are applied to every bearing location individually. To correctly reproduce the load behavior of unbalance forces, two forces per bearing location were used including a phase shift between them

$$F_{\mathrm{y}} = \hat{F} \cdot \sin\left(2 \cdot \pi \cdot f\right) \quad [\mathrm{N}] \quad (3)$$

$$F_{\mathrm{z}} = \hat{F} \cdot \sin\left(2 \cdot \pi \cdot f + 270°\right) \quad [\mathrm{N}] \quad (4)$$

with the amplitudes of the individual bearing unbalance forces $\hat{F}$ [N] and the excitation frequency f [Hz]. This results in a circulatory excitation of the bearing locations in the y-z-plane once the system reaches steady state, see Figure 5. Every individual rotor induces unbalance

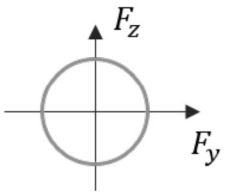

Figure 5: Representation of load behavior on bearing locations due to unbalance forces

forces at its respective rotation speed on the bearings. Currently, it is assumed that all unbalance forces of an individual rotor run in-phase. This is a conservative assumption as this results in the biggest possible excitation.

The mass of the pylon is considered based on its geometry and the material parameters for aluminium. However, the engine structure needs to be augmented with point masses in order to include the mass of the actual engine and rotors. The rotor masses are known from the engine layout data sheet mentioned in the chapter *Estimation of Engine Vibrations* and the total mass of the engine from the V2500 maintenance documents [4]. Each bearing location gets a point mass assigned which includes the fractional rotor mass for the bearing based on the fractional load factor from Equation (2) and the average engine casing mass per bearing location

$$m_{\mathrm{LP\ bearing,i}} = m_{\mathrm{LP\ Rotor}} \cdot k_{\mathrm{LP,i}} \quad [\mathrm{kg}] \quad (5)$$

$$m_{\mathrm{HP\ bearing,i}} = m_{\mathrm{HP\ Rotor}} \cdot k_{\mathrm{HP,i}} \quad [\mathrm{kg}] \quad (6)$$

$$m_{\mathrm{casing\ avg}} = \frac{m_{\mathrm{engine}} - m_{\mathrm{LP\ Rotor}} - m_{\mathrm{HP\ Rotor}}}{n_{\mathrm{bearings}}} \quad [\mathrm{kg}] \quad (7)$$

$$m_{\mathrm{LP\ bearing\ total,i}} = m_{\mathrm{LP\ bearing,i}} + m_{\mathrm{casing\ avg}} \quad [\mathrm{kg}] \quad (8)$$

$$m_{\mathrm{HP\ bearing\ total,i}} = m_{\mathrm{HP\ bearing,i}} + m_{\mathrm{casing\ avg}} \quad [\mathrm{kg}] \quad (9)$$

In case of the V2500 jet engine the following values apply: $n_{bearings} = 5$, $m_{LP\ Rotor} = 404$ kg, $m_{HP\ Rotor} = 246$ kg, $m_{engine} = 2300$ - 2400 kg (dry).

The FEM model is calculated in time-domain utilizing NASTRANs Direct Transient Frequency Response solution sequence. The time-domain calculation is necessary as there are multiple forces with different frequencies

and phase-shifts exciting the system simultaneously. The time-domain results are transformed to the frequency-domain using the Fast-Fourier-Transformation (FFT).

Results

The results are force and moment spectra. An example of the force spectra for the attachment point at the back of the pylon to the wing in y-direction can be seen in Figure 6. The four considered frequencies (0.5 x N_1, N_1, 2 x N_1, N_2) can be clearly identified. The proportions between the force amplitudes vary according to their impact at the respective location. Comparing the example spectrum to

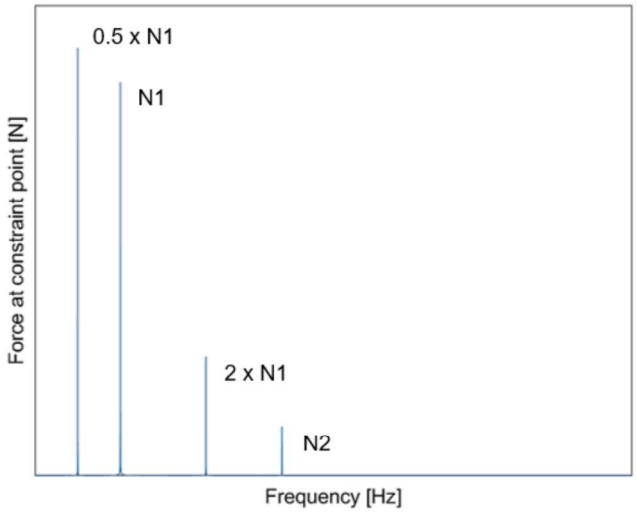

Figure 6: Force spectrum for the rear attachment point of the pylon to the wing in y-direction

spectra of other directions it becomes apparent that the model fulfills its tasks and distributes the loads accordingly. Figure 7 shows a bar chart with all force spectra for the front and rear attachment point of the pylon in y- and z-direction. The moment spectrum about the x-axis at the forward attachment point between pylon and wing showed neglect-able values compared to the force spectra. Over all locations the force amplitudes are not

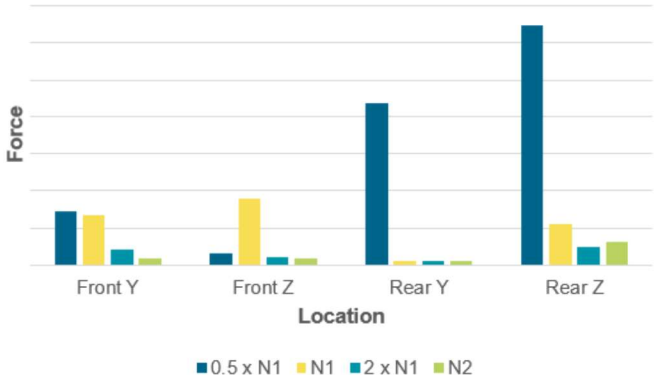

Figure 7: Force spectrum for the rear attachment point of the pylon to the wing in y-direction

evenly distributed. The spectra for both directions in the rear of the pylon show clearly that the highest forces are transmitted at the sub-harmonic 0.5 x N1. In case of both directions in the front the sub-harmonic 0.5 x N1 and N1 itself dominate the force transmission. An explanation for the rear forces might be the fact that the excitation forces at the bearing locations create a significant moment of force that must be compensated with large support forces at the back of the pylon.

Conclusion & Outlook

The goal of this work was to create a simple model to estimate the load spectra in the interface between pylon and wing. These estimated load spectra shall act as input for numerical models of aircraft structures but also for experiments on respective structures. As there are no detailed measurement data available in this interface, available relevant data from different sources of the DLR was gathered and basic theoretical assumptions were used.

The model generates physically reasonable results. The spectra for the different attachment points between pylon and wing show dissimilar force ratios. Therefore, the models seems to result in load cases which make sense considering the structure of the engine-pylon-wing system. However, the model is built-up mostly on theoretical assumptions. Thus, no judgment can be made as to how realistic the resulting spectra actually are. So far there are no measurement results of a respective system available and thus the numerical data cannot be validated.

The following possibilities would allow to either improve the model accuracy or perform a validation. One possibility would be to include a detailed FEM model of the jet-engine core structure. Applying the calculated unbalance loads on the bearing locations of such a more sophisticated model would result in more realistic spectra. The second possibility would be to validate the model with data from a blocked force measurement on a respective system [6]. The DLR is currently planning such a measurement on one of its research aircrafts.

References

[1] Deutsches Institut für Normung e.V. (2004). Mechanical vibration - Balance quality requirements for rotors in a constant (rigid) state - Part 1: Specification and verification of balance tolerances (ISO 1940-1:2003).

[2] Norambuena, M., Böswald, M., Govers, Y. (2016). Vibro-acoustic analysis of flight test data comprising fuselage vibrations, external pressure and interior cabin noise measurements. 54th AIAA Aerospace Sciences Meeting, San Diego.

[3] Engine-Pylon and Pylon-Wing Interface, URL: `https://upload.wikimedia.org/wikipedia/commons/3/3e/DC-10_engine-pylon.svg`

[4] IAE V2500 General Familiarisation (2000). IAE International Aero Engines AG.

[5] Biedermann, J., et al. (2017). Classification of the mid-frequency range based on spatial Fourier decomposition of operational deflection shapes. 24th ICSV, 2017. London.

[6] Moorhouse, A.T., Elliott, A.S., Evans, T.A. (2009). In situ measurement of the blocked force of structure-borne sound sources. Journal of Sound and Vibration, 325, 679-685.